

Research Article

Global proteome of *LonP1*^{+/-} mouse embryonal fibroblasts reveals impact on respiratory chain, but no interdependence between Eral1 and mitoribosomes

Jana Key¹, Aneesha Kohli¹, Clea Bárcena², Carlos López-Otín², Juliana Heidler³, Ilka Wittig^{3,*}, and Georg Auburger^{1,*}

¹ Experimental Neurology, Goethe University Medical School, 60590 Frankfurt am Main;

² Departamento de Bioquímica y Biología Molecular, Facultad de Medicina, Instituto Universitario de Oncología (IUOPA), Universidad de Oviedo, 33006 Oviedo, Spain;

³ Functional Proteomics Group, Goethe-University Hospital, 60590 Frankfurt am Main, Germany

* Correspondence: wittig@med.uni-frankfurt.de; auburger@em.uni-frankfurt.de

Abstract: Research on healthy ageing shows that lifespan reductions are often caused by mitochondrial dysfunction. Thus, it is very interesting that the deletion of mitochondrial matrix peptidase LonP1 was observed to abolish embryogenesis, while deletion of the mitochondrial matrix peptidase ClpP prolonged survival. To unveil the targets of each enzyme, we documented the global proteome of *LonP1*^{+/-} mouse embryonal fibroblasts (MEF), for comparison with *ClpP*^{-/-} depletion. Proteomic profiles of *LonP1*^{+/-} MEF generated by label-free mass spectrometry were further processed with the STRING webserver Heidelberg for protein interactions. ClpP was previously reported to degrade Eral1 as a chaperone involved in mitoribosome assembly, so ClpP deficiency triggers accumulation of mitoribosomal subunits and inefficient translation. *LonP1*^{+/-} MEF also showed Eral1 accumulation, but no systematic effect on mitoribosomal subunits. In contrast to *ClpP*^{-/-} profiles, several components of the respiratory complex I membrane arm were accumulated, whereas the upregulation of numerous innate immune defense components was similar. Overall, LonP1 as opposed to ClpP appears to have no effect on translational machinery, instead it shows enhanced respiratory dysfunction; this agrees with reports on the human CODAS syndrome caused by LonP1 mutations.

Keywords: longevity; life expectancy; CODAS syndrome; Perrault syndrome; protease target substrates; respiratory complex assembly; oxidative stress; glutathione pathway; lysosomal degradation; fidelity protein synthesis

1. Introduction

Mitochondria are double membraned subcellular organelles which are implicated in multiple cellular processes. In addition to their main role in the production of energy through being the organelle housing oxidative phosphorylation, mitochondria exert many other functions. These range from cellular calcium homeostasis [1], regulation of reactive oxygen species (ROS), assembly of iron-sulfur-cluster and heme, to participation in innate immune responses of any cell type. Respecting their manifold roles mitochondria have been shown to play important roles in various diseases, such as neurodegenerative diseases [2], inflammatory damage [3, 4] and cancer [5, 6].

Within mitochondria there are several energy (ATP)-dependent proteolytic systems. Next to DJ-1, PARL, Yme1 and mAAA-proteases around the mitochondrial intermembrane space, they include two proteases that are localized in the mitochondrial matrix, namely LonP1 (Lon Protease Homolog) and ClpP (Caseinolytic Mitochondrial Matrix Peptidase Proteolytic Subunit) [2, 7]. Their exact role in humans is not fully understood up to date. However, there are many more other proteases that contribute to cellular proteostasis, inside and outside of mitochondria. Mutations in the mAAA protease Afg3l2 in the mitochondrial inner membrane was shown to cause dominant hereditary ataxia SCA28 [8]. Mutations in the peptidase and redox-dependent molecular chaperone DJ-1 that inhibits α -synuclein aggregate formation are the cause of autosomal recessive Parkinsonism (PARK7) [9]. PARL in the inner mitochondrial membrane is responsible for the stress-dependent degradation of PINK1, whose mutation affects mitochondrial turnover via Parkin-dependent mitophagy, where other variants of hereditary Parkinsonism named PARK6 and PARK2 are triggered [10-19].

Mitochondrial dysfunction is often related to a change of lifespan [20, 21]. Using the survival of cells and organisms as criteria, it seems clear that LonP1 is the main mitochondrial matrix protease given that its deficiency results in embryonic lethality [6]. In contrast, ClpP seems to play an accessory role in stress response, with its deficiency even extending lifespan in some fungus named *Podospora anserina* [22].

LonP1 is an AAA+ (ATPase associated with various cellular activities) domain containing, highly conserved serine peptidase, functioning as protease, chaperone and interactor of single-stranded mitochondrial DNA [23-26]. It has been shown to be responsible for the degradation of misfolded or damaged proteins and for the assembly of respiratory chain complexes [27]. Point mutations of LonP1 in humans lead to the development of a rare disease named CODAS syndrome (cerebral, ocular, dental, auricular, and skeletal syndrome) with failure of oxidative phosphorylation [28-30].

LonP1 has been described to degrade several proteins within the mitochondrial matrix, such as mitochondrial Aconitase [24], a Cytochrome *c* oxidase subunit (Cox4-1) [31], Mitochondrial Steroidogenic Acute Regulatory (StAR) Protein [32], Alas1, the rate-limiting enzyme in heme biosynthesis [33], and phosphorylated Tfam as a mitochondrial transcription factor [34]. A systematic global survey of its degradation substrates, their half-life changes and possible compensatory efforts has not been carried out.

ClpP in the mitochondrial matrix is also a highly conserved serine peptidase, which is assembled in a barrel-like structure together with ClpX, the latter one providing energy via its ATPase function and assuring substrate specificity [35]. ClpP has been shown to play a role in the unfolded protein response in mitochondria (UPRmt) in *C. elegans* and may play a role in the degradation of unfolded proteins in rodents as well as in humans [36-38]. Mutations in ClpP in humans lead to the development of Perrault syndrome 3 (PRLTS3), which is modeled by ClpP^{-/-} mice that mirror the infertility, sensorineural hearing loss, ataxia and growth retardation known from PRLTS3 patients [39, 40]. In addition, mitochondrial DNA (mtDNA) content was shown to be present in excess in the absence of ClpP. It was shown recently that ClpP deficiency impairs the fidelity of mitochondrial translation and leads to an accumulation of mitoribosomes. This is thought to be caused by the pathological accumulation of the mitoribosomal assembly factor ERAL1, which was claimed to be a direct proteolytic substrate of ClpP [41].

While on one hand, the deficiency of LonP1 and subsequent accumulation of misfolded proteins in the mitochondria trigger an increase of PINK1 and the engulfment/elimination of mitochondria via autophagy [42], on the other hand, the deficiency of ClpP triggers selective changes in the cytosolic proteasome [40]. In both cases, the mitochondrial dysfunction caused by either LonP1 or ClpP depletion activate the RIG-1-like receptor pathway of the innate immune system, perhaps simply by altered binding of lactate and hexokinase-2 to the mitochondrial antiviral signaling protein Mavs [40, 43-45]. In order to elucidate the pathology of mitochondrial proteostasis and the compensatory efforts of the surrounding cell in further detail, we used *LonP1*^{+/-} mouse embryonic fibroblasts to document their global proteome profile. The comparison with previously reported *ClpP*^{-/-} expression profiles may help to identify substrates that are selectively degraded by one of these proteases.

2. Results

The analysis of previously generated [6] *LonP1*^{+/-} MEFs versus wildtype littermate MEFs regarding their global proteome profile by quantitative label-free mass spectrometry detected a total of 5,929 proteins. A high number exhibited significant changes in abundance (Suppl. Table A1). Among them, 463 proteins were significantly upregulated and 328 downregulated. Thus, despite the deficiency of the main mitochondrial protease in these cells, there was no strong bias towards protein accumulations in the profile. However, the effects were clearly non-random, with highly significant enrichments of specific pathways and an overall protein-protein-interaction enrichment p-value of <1.0e-16 upon bioinformatics analysis at the STRING webpage in Heidelberg. Interestingly, known *LonP1* degradation targets such as *Tfam* and *Aco2* [46-48] did not show significantly elevated abundance in this heterozygous *LonP1* depletion state. It is also noteworthy that indicators of mitochondrial biogenesis such as *Ppargc1a*, *Nrf1*, *Nrf2*, *Tfam* [49] or components of the selective autophagy for mitochondria such as *Pink1*, *Park2*, *Bnip3*, *Bnip3l*, *Fundc1*, *Ambra1*, *Mul1*, *Arih1*, *March5*, *gp78/Amfr*, *Mgrn1* and *Huwe1* [50, 51] did not show dysregulated abundance. With regard to the selectivity of proteolytic degradation by *LonP1* versus *ClpXP* in the mitochondrial matrix, it is important to note that mitoribosomal subunits were not accumulated in *LonP1*^{+/-} MEFs, in contrast to *ClpP*^{-/-} proteome profiles.

Among the upregulated factors, enrichment analyses with STRING highlighted the KEGG pathway of “lysosome” (false discovery rate FDR = 8.75e-12) and the REACTOME pathways “neutrophil degranulation” (FDR = 1.08e-16) and “innate immune system” (FDR = 1.94e-12).

Among the downregulated factors, STRING enrichment analyses highlighted the KEGG pathway “focal adhesion” (FDR = 2.82e-12), the REACTOME pathway “cell junction organization” (FDR = 4.21e-06) and the INTERPRO domain features “zinc finger, LIM type” (FDR = 3.08e-06).

The distribution of dysregulations and the most important factors are illustrated in a volcano plot (Figure 1), where the genetically reduced abundance of *LonP1* is illustrated with a blue dot, other significant downregulations are shown in green, and the relevant upregulations in red color. The strongest significant downregulation concerned *Trim44*, as a modulator of glycolysis together with lactate production, and as a modulator of inflammation via interaction with *Mavs* [44, 52, 53]. The strongest significant upregulations concerned several components of immune pathways such as *Igsf1*, *Kdelr1*, *Lgals3bp*, but importantly, also a crucial defense factor against oxidative stress, namely *Cat* (catalase). Its induction probably has compensatory nature, given that it is known to protect mitochondrial energetics in the face of *LonP1* deficiency [54].

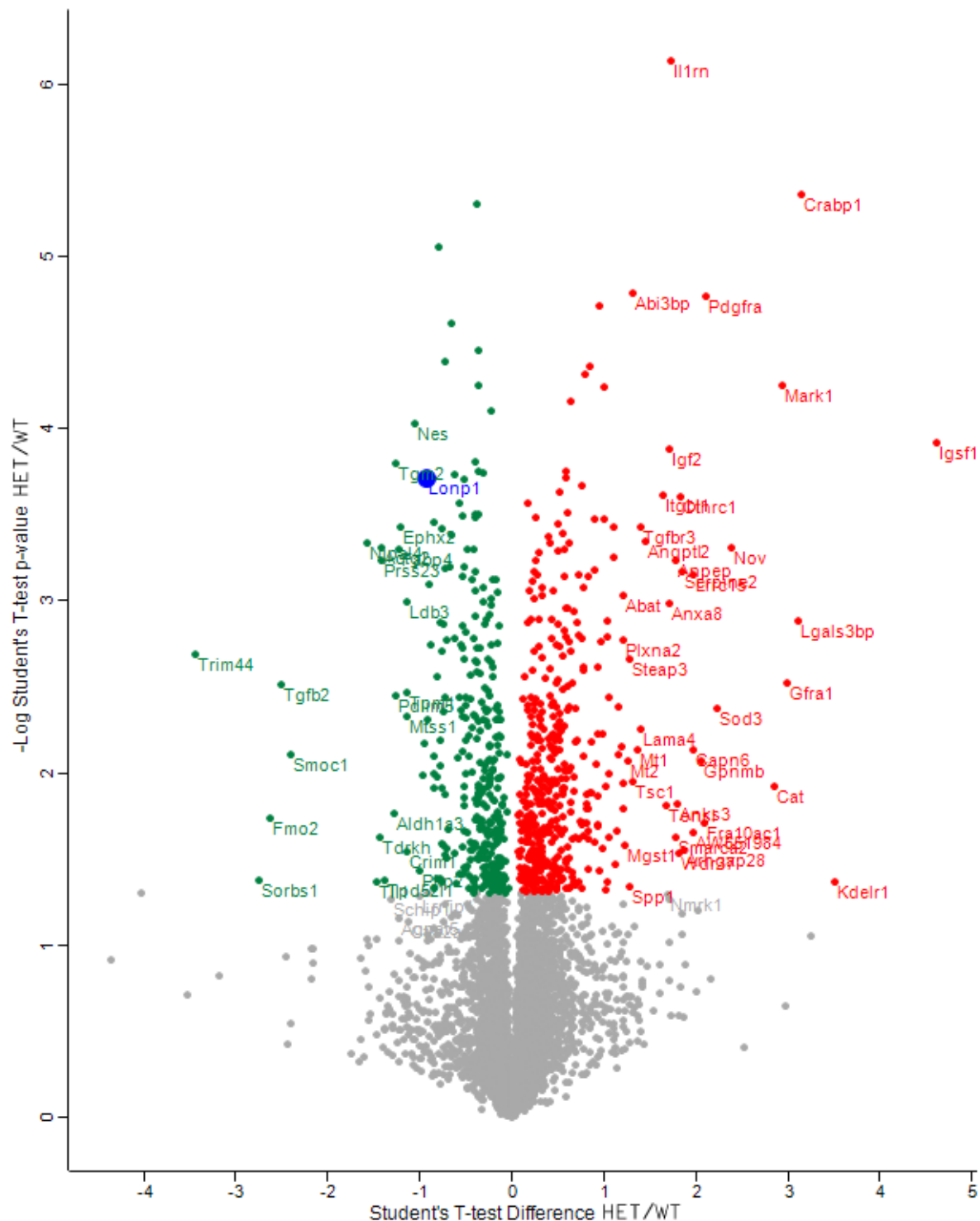


Figure 1: This Volcano plot represents all significant dysregulations in the global proteome of *LonP1*^{+/−} MEFs (HET) in green color (downregulated), red color (upregulated) or blue color (genetically deleted). The two-fold deficiency of LonP1 is represented by log-2 values as -1 on the X-axis. Significance values are shown on the Y-axis. Peptides with non-significant changes are shown as grey dots. Factors of high significance despite moderate fold-change such as LonP1 can be easily distinguished in this diagram from other factors of massive fold-changes with higher variability such as the longevity and health span factor Fmo2 [55].

2.1. Dysregulated mitochondrial factors in LonP1^{+/-} MEFs are enriched for oxidation processes

To understand how LonP1 deficiency triggers these cellular responses, we selected among all significant dysregulations only those factors that are enriched in mitochondria, based on their classification in the STRING database and the localization predictions in the GeneCards database (see Table 1).

Protein names	Gene names	p-value	fold change
Lon protease homolog, mitochondrial	<i>Lonp1</i>	1.92E-04	-1.92
Dihydroorotate dehydrogenase (quinone), mitochondrial	<i>Dhodh</i>	2.19E-02	-1.44
Amine oxidase [flavin-containing] A	<i>Maoa</i>	7.93E-03	-1.38
Solute carrier family 25 member 46	<i>Slc25a46</i>	4.42E-02	-1.21
Mitochondrial-processing peptidase subunit beta	<i>Pmpcb</i>	1.21E-02	-1.19
28S ribosomal protein S2, mitochondrial	<i>Mrps2</i>	4.23E-02	-1.18
60 kDa heat shock protein, mitochondrial	<i>Hspd1</i>	3.52E-03	-1.18
Voltage-dependent anion-selective channel protein 2	<i>Vdac2</i>	4.61E-02	-1.12
NADH dehydrogenase [ubiquinone] 1 alpha subcomplex subunit 5	<i>Ndufa5</i>	3.12E-02	-1.09
Mitochondrial import receptor subunit TOM70	<i>Tomm70a</i>	1.96E-02	-1.08
C-1-tetrahydrofolate synthase,	<i>Mthfd1</i>	4.26E-02	-1.08
Monofunctional C1-tetrahydrofolate synthase, mitochondrial	<i>Mthfd1l</i>	4.96E-02	-1.05
4-aminobutyrate aminotransferase, mitochondrial	<i>Abat</i>	9.25E-04	2.32
Calcium uptake protein 2, mitochondrial	<i>Micu2</i>	4.11E-03	2.24
Monocarboxylate transporter 1	<i>Slc16a1</i>	2.40E-03	1.72
Pyruvate carboxylase;Pyruvate carboxylase, mitochondrial	<i>Pcx;Pc</i>	7.33E-03	1.43
Carnitine O-palmitoyltransferase 2, mitochondrial	<i>Cpt2</i>	3.01E-03	1.39
Oxidation resistance protein 1	<i>Oxr1</i>	4.71E-03	1.36
Mitochondrial chaperone BCS1	<i>Bcs1l</i>	1.27E-02	1.32
Mitochondrial 2-oxoglutarate/malate carrier protein	<i>Slc25a11</i>	1.08E-02	1.28
Nucleoside diphosphate-linked moiety X motif 8, mitochondrial	<i>Nudt8</i>	4.73E-02	1.25
Propionyl-CoA carboxylase beta chain, mitochondrial	<i>Pccb</i>	3.92E-03	1.24
Ferrochelatase;Ferrochelatase, mitochondrial	<i>Fech</i>	4.74E-03	1.23
Probable arginine--tRNA ligase, mitochondrial	<i>Rars2</i>	2.34E-02	1.22
AFG3-like protein 2	<i>Afg3l2</i>	1.28E-02	1.21
NADH dehydrogenase [ubiquinone] 1 alpha subcomplex subunit 10, mitochondrial	<i>Ndufa10</i>	3.08E-02	1.20
GTPase Era, mitochondrial	<i>Eral1</i>	1.97E-03	1.18
Peptidyl-tRNA hydrolase 2, mitochondrial	<i>Pthr2</i>	3.60E-02	1.18
NADH dehydrogenase [ubiquinone] 1 beta subcomplex subunit 7	<i>Ndufb7</i>	1.81E-02	1.15
NADH dehydrogenase [ubiquinone] 1 beta subcomplex subunit 4	<i>Ndufb4</i>	2.52E-02	1.12
Calcium-binding mitochondrial carrier protein Aralar1	<i>Slc25a12</i>	1.57E-02	1.12
Mitochondrial amidoxime reducing component 2	<i>Marc2</i>	1.91E-02	1.12
Isocitrate dehydrogenase [NADP], mitochondrial	<i>Idh2</i>	4.92E-02	1.11
Phosphoenolpyruvate carboxykinase [GTP], mitochondrial	<i>Pck2</i>	3.71E-03	1.09

Table 1: List of mitochondrial factors with significant dysregulation, ordered by direction of change (dark green color for downregulations, red for upregulations) and by fold-changes. In response to the deficiency of the AAA+ domain containing peptidase LonP1 (purple), several AAA+ domain containing factors and proteases (highlighted in yellow) as well as two chaperones (orange) were altered. Several subunits of the respiratory complex I stood out (green), with upregulations of three subunits in the membrane arm (P module) [56] and one subunit in the matrix arm of iron/sulfur and flavoproteins (NQ modules) showed a minor downregulation.

In a STRING analysis to identify regulated pathways (enrichment p-value <1.0e-16), the changes concerned inner membrane factors (FDR = 3.81e-15) even more strongly than the mitochondrial matrix factors (FDR = 3.37e-12), in particular the Biological Process GO term “oxidation-reduction” (FDR = 5.33e-10). Among the KEGG and REACTOME pathways, the “Complex-I biogenesis” (FDR = 5.14e-05) and the “Processing of SMDT1” (FDR = 5.52e-05) as inner membrane processes were affected more significantly than the matrix processes “citrate cycle” (FDR = 4.30e-04) and gluconeogenesis (FDR = 2.50e-04). Also in the matrix, the one-carbon metabolism was affected with “formate-tetrahydrofolate ligase” being prominent among PFAM protein domains (FDR = 9.60e-4), while membrane processes again dominated with “mitochondrial carrier protein superfamily” (FDR = 2.0e-04) among INTERPRO

protein domains, and the dysregulation of several AAA+ disaggregases appeared as “ATPases associated with a variety of cellular activities” (FDR =2.09e-02) among SMART protein domains in response to deficiency of the AAA+ domain containing LonP1. Figure 2 illustrates these factors with various colors for each pathway, and with connecting lines that represent different evidence for interactions among them. Importantly, respiratory complex I subunits in the ND5, ND4 and ND2 module of the membrane arm accumulate, in contrast to a subunit from the Q module in the hydrophilic peripheral arm in the mitochondrial matrix. Overall, complex-I assembly stoichiometry appears to be more strongly affected by LonP1 deficiency than the previously reported LonP1-dependent degradation substrates such as Tfam or Aco2.

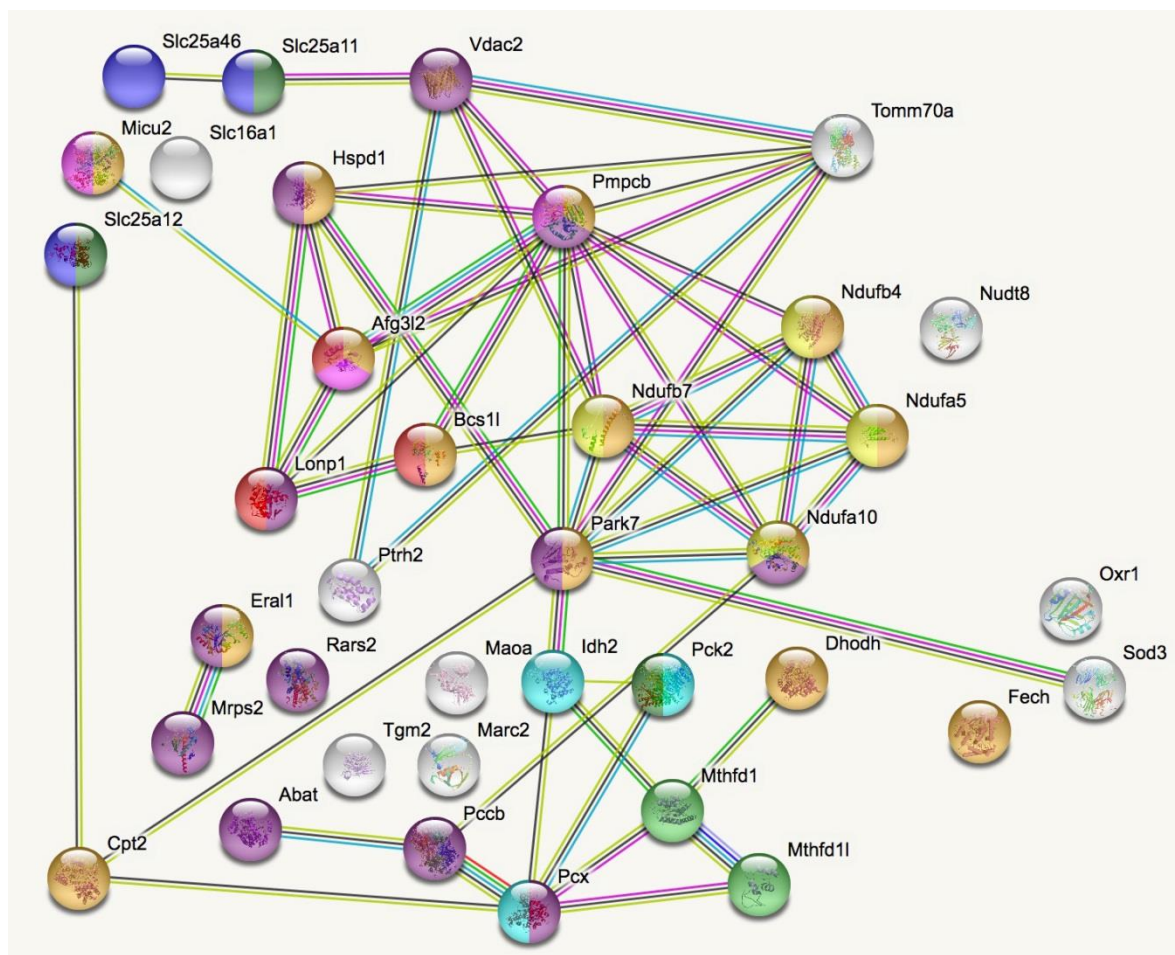


Figure 2: The STRING diagram of protein-protein interactions shows all significant dysregulations in mitochondria. In colors it highlights mitochondrial matrix factors (violet), inner membrane proteins (orange), TCA cycle (light blue), gluconeogenesis (dark green), complex-I biogenesis (yellow), processing of Smdt1 (pink), formate-tetrahydrofolate ligase (light green), mitochondrial carrier domain superfamily (dark blue) and AAA+ ATPases (red). The membrane carriers and pore factors were manually placed in the left upper corner and upper margin, while the respiratory complex components were positioned in the right upper corner. LonP1 and its interaction with other disaggregases, proteases and chaperones were located in the middle from left to center. The Eral1 mitoribosome chaperone and other translation components are shown towards the lower left corner, the breakdown of fatty acids / amino acids / one-carbon flux towards the lower center, and oxidative stress response in the lower right corner.

2.1.1. Mitochondrial downregulations in LonP1^{-/-} MEFs

In parallel with the deficiency of LonP1, strongly significant reductions appeared (Table 1) for the chaperone Hspd1, which is responsible of folding mitochondrial proteins to their native state [57], and for the peptidase Pmpcb (beta-MPP), which catalyzes the cleavage of mitochondrial precursor

proteins upon import, before they are folded [58, 59]. In addition, a strongly significant reduction of the Tomm70a import receptor in the outer membrane translocase suggests that the recruitment and folding of precursor proteins decrease massively. Three components of the nucleobase biosynthetic process were also diminished with strong significance, namely Dhodh as the only mitochondrial factor involved in *de novo* pyrimidine synthesis, as well as Mthfd1l and Mthfd1 as mitochondrial factors involved in *de novo* purine synthesis. This suggests that RNA and DNA processes in LonP1^{+/-} mitochondria may become unbalanced.

2.1.2 Mitochondrial upregulations in LonP1^{+/-} MEFs

The most prominent increase among mitochondrial factors (Table 1) concerned the transaminase Abat, which cooperates with the succinate-CoA ligases Suc1g1 and Suc1a2 to convert dNDPs to dNTPs, while also affecting the glutamate-glutamine cycle and mediating the GABA-shunt as a complement to the TCA cycle that is crucial for anoxia and acid tolerance [60-62]. The second most significant upregulation was noted for the mitoribosome assembly factor Eral1. This was a surprising finding, given that Eral1 was recently claimed to be a selective substrate of ClpXP-mediated degradation [41]. ClpP protein levels were unchanged in LonP1^{+/-} MEF (Suppl. Table A1), ruling out that this effect was still dependent on ClpP. In a subsequent paragraph, we performed meta-analyses of two published proteome profiles in comparison to this proteome profile to assess the questions, whether mitoribosome accumulation is a ClpXP-specific effect, whether Eral1 accumulation is a ClpXP-specific effect or also depends on the presence of LonP1, and whether mitoribosome and Eral1 levels depend on each other.

Several other upregulated factors in LonP1^{+/-} MEFs reflect enhanced oxoacid metabolism in the mitochondrial matrix, namely Pcx, Pck2, Pccb, Idh2, Cpt2, Marc2 and Rars2. The increased levels of Fech and Oxr1 presumably imply efforts to compensate oxidative stress within mitochondria. Importantly, the deficiency of the AAA+ domain containing peptidase LonP1 triggered elevated levels for two factors with a role in protein processing: Firstly, Bcs1l as a AAA+ domain-containing assembly factor of respiratory complex-III accumulated [63]. Secondly, an accumulation was found for the AAA+ domain containing peptidase Afg3l2 (mAAA-subunit-2), which modulates assembly of respiratory complex-IV and of the MCU complex [64, 65]. Both are highlighted in yellow in Table 1. Overall, many upregulations refer to oxoacid metabolism, oxidative stress and assembly of the oxidative phosphorylation / respiratory chain.

2.1.3 Eral1 and mitoribosomal factors as substrates of LonP1 versus ClpXP – two meta-analyses:

In an effort to understand to what degree the degradation of the RNA-chaperone Eral1 is due to LonP1 or ClpXP, and whether Eral1 accumulation is prominently responsible for the assembly of the 28S ribosomal subunit in mitochondria, we reassessed previously published global proteome data from the heart of *ClpP*^{-/-} mice [41]. Highly significant peptide accumulations were observed not only for Eral1, but also for several other mitochondrial matrix chaperones. In particular, a massive increase was observed for ClpX (91.8-fold, $p = 3.8 \times 10^{-5}$). Substantially elevated levels existed also for Trap1 (4.8-fold, $p = 7.11 \times 10^{-6}$), Grpel1 (3.5-fold, $p = 7.03 \times 10^{-6}$), Hspa9 (2.5-fold, $p = 1.4 \times 10^{-5}$) and Dnaja3 (2.1-fold, $p = 3.6 \times 10^{-4}$). It remained unclear to what degree excessive transcriptional induction versus deficient proteolytic turnover is responsible for these chaperone accumulations [41]. Thus, a host of chaperones show elevated levels in parallel to the mitoribosome accumulation.

In view of the massive ClpX accumulation above, it is also interesting to re-assess a recent study where ClpX had been overexpressed 1.8-fold in C2C12 mouse myoblast cells and the global proteome profile was documented [36]. While ClpX is elevated in both experiments, ClpP as an interactor protein showed a 1.4-fold co-accumulation upon ClpX overexpression, in contrast to the previous ClpP deletion study. Thus, a comparison of both profiles permits the identification of selective consequences of ClpP deficiency versus ClpP overactivity, separating them from indirect effects. We

performed an analogous bioinformatics assessment of this published dataset, selecting the proteins with >1.5-fold accumulation and testing their pathway interaction profile in STRING enrichment statistics and diagrams. Indeed, the STRING diagram of upregulations upon ClpX overexpression (Suppl. Fig. A1) detects similarly strong accumulations of mitoribosomal subunits as in *ClpP*^{-/-} tissues with their massive ClpX accumulation. Thus, strong mitoribosomal accumulation occurs in both cases together with elevated ClpX levels. In contrast, Era1 levels showed only 1.1-fold upregulation in ClpX overexpression myoblasts. The most significant findings in ClpX overexpression myoblasts (see Suppl. Table A2) reflect mitochondrial and nucleolar anomalies, with altered ribosome biogenesis. Relevant similarities include the co-accumulation of Noa1 (1.7-fold), Hspa9 (1.5-fold) and Grpel2 (1.4-fold) with ClpX. The increased levels of many chaperones might simply be due to co-accumulation with misfolded mitochondrial ribosome complexes. Specifically, Era1 may simply show retarded turnover upon accumulation of its binding partners, mitoribosomes and RNAs. Overall, the available data suggest that the accumulation of mitoribosomes in *ClpP*^{-/-} tissues depends on elevated ClpX levels and is independent from Era1 accumulation. In contrast to mitoribosomes, Era1 levels are not determined by ClpX-mediated degradation alone, but affected in ClpP deficiency, in ClpX overexpression, and in LonP1 deficiency.

2.2. Oxidative stress and glutathione pathways in *LonP1*^{+/-} MEFs

Beyond the mainly mitochondrial factors, relevant enrichments among GO terms Biological processes were noted for “response to oxidative stress” (FDR = 0.00060) and “glutathione metabolic process” (FDR = 0.00055) in the *LonP1*^{+/-} MEF proteome profile, with an upregulation for each of these enzymes except the glutathione synthase Gss, the spermine synthase Sms and the hypoxia-inducible factor Egl1 (Table 2). These upregulations were strongest for Cat and Mgst1, which are present both in mitochondria and the cytosol, and small for Gstm5 and Gstm2 whose mitochondrial presence is weak, according to localization predictions in the GeneCards database. It seems likely that these changes are secondary to the altered oxidative processes within mitochondria.

Protein names	Gene names	p-value	fold change
Catalase	<i>Cat</i>	1.20E-02	7.22
Superoxide dismutase [Cu-Zn]; Extracellular superoxide dismutase [Cu-Zn]	<i>Sod3</i>	4.22E-03	4.67
Aminopeptidase N	<i>Anpep</i>	5.87E-04	3.44
Microsomal glutathione S-transferase 1	<i>Mgst1</i>	2.61E-02	2.35
Glutathione S-transferase A4	<i>Gsta4</i>	1.21E-02	2.02
Lactoylglutathione lyase	<i>Glo1</i>	4.32E-02	1.65
Nicotinate phosphoribosyltransferase	<i>Naprt</i>	4.69E-02	1.50
Glutathione S-transferase omega-1	<i>Gsto1</i>	1.36E-03	1.41
Glutathione S-transferase Mu 5	<i>Gstm5</i>	3.56E-02	1.39
Serine/threonine-protein kinase 24; Serine/threonine-protein kinase 24 35 kDa subunit; Serine/threonine-protein kinase 24 12 kDa subunit	<i>Stk24</i>	4.92E-03	1.25
Isocitrate dehydrogenase [NADP]; Isocitrate dehydrogenase [NADP] cytoplasmic	<i>Idh1</i>	1.52E-02	1.23
Maleylacetoacetate isomerase	<i>Gstz1</i>	1.24E-02	1.19
Glutathione S-transferase Mu 2	<i>Gstm2</i>	3.67E-03	1.16
Isocitrate dehydrogenase [NADP], mitochondrial	<i>Idh2</i>	4.92E-02	1.11
Protein deglycase DJ-1	<i>Park7; Dj1</i>	2.07E-02	1.10
Glutathione synthetase	<i>Gss</i>	1.52E-02	-1.25
Spermine synthase	<i>Sms</i>	1.38E-02	-1.29
Egl nine homolog 1	<i>Egln1</i>	2.86E-02	-1.23
Catalase	<i>Cat</i>	2.25E-02	-1.20

Table 2: List of dysregulated factors in the oxidative stress and antioxidant glutathione pathways, ordered by direction of change (red for upregulations, dark green for downregulations) and by fold-changes. The strongest upregulation was observed for the heme-iron-binding catalase (Cat), while another Cat peptide showed minor downregulation.

2.3 Activation of the innate immune system in *LonP1^{+/-}* MEFs

In the STRING analysis of all enrichments among REACTOME pathways, “neutrophil degranulation” (FDR = 3.16e-15) and “innate immune system” (FDR = 4.26e-11) were prominent. Among the individual dysregulations, the strongest effect was an ~11-fold downregulation of Trim44 (Table 3), which is responsible for stabilizing Mavs as the mitochondrial antiviral signaling factor [53]. Weaker downregulations concerned several Cluster of Differentiation (CD) antigens, namely CD44, CD97, CD109 and CD302. This is in good agreement with recent observations that dysfunctional mitochondria will release toxic dsRNA and mtDNA [66, 67]. Indeed, within the innate immune system there was an upregulation of cytosolic sensor pathway components, both for the detection of toxic RNA (namely *Ifi35*, *Ifih1*, *Tspan6*, *Eif2ak2*, *Trim25*) and toxic DNA (*Ifi204*, *Tmem173*/STING, *Mnda*). Examining the subset of immunity-related dysregulations in a further STRING analysis, significant enrichments were detected for “response to cytokine” (FDR = 5.01e-07), “defense response to virus” (FDR = 8.94e-07), “Jak-Stat signaling pathway” (FDR = 0.00044), “NOD-like receptor signaling pathway” (FDR = 0.00044) and “RIG-I-like receptor signaling pathway” (FDR = 0.00044).

Protein names	Gene names	p-value	fold change
Transmembrane glycoprotein NMB	<i>Gpnmb</i>	8.44E-03	4.17
Interleukin-1 receptor antagonist protein	<i>Il1rn</i>	7.28E-07	3.32
Osteopontin	<i>Spp1</i>	4.53E-02	2.42
Lymphocyte antigen 6A-2/6E-1	<i>Ly6a</i>	7.74E-03	2.23
Atypical chemokine receptor 3	<i>Ackr3</i>	2.44E-03	1.92
Coxsackievirus and adenovirus receptor homolog	<i>Cxadr</i>	5.89E-03	1.91
Interferon-activable protein 204	<i>Ifi204</i>	2.54E-02	1.86
H-2 class I histocompatibility antigen, D-B alpha chain	<i>H2-D1;H-2D;H2-L</i>	1.29E-02	1.82
H-2 class I histocompatibility antigen, K-K alpha chain;	<i>H2-K1;H2-K;H2-D1</i>	1.29E-02	1.81
Tetraspanin;CD82 antigen	<i>Cd82</i>	4.35E-05	1.80
Signal transducer and activator of transcription;Signal transducer and activator of transcription 2	<i>Stat2</i>	2.43E-02	1.77
Interferon-induced 35 kDa protein homolog	<i>Ifi35</i>	3.65E-02	1.77
Interferon-induced helicase C domain-containing protein 1	<i>Ifih1</i>	2.34E-02	1.61
Tetraspanin;Tetraspanin-6	<i>Tspan6</i>	1.28E-02	1.60
Gamma-interferon-inducible lysosomal thiol reductase	<i>Ifi30</i>	1.16E-03	1.59
Signal transducer and activator of transcription;Signal transducer and activator of transcription 1	<i>Stat1</i>	2.70E-02	1.53
Stimulator of interferon genes protein, STING	<i>Tmem173</i>	1.55E-02	1.44
Interferon-induced, double-stranded RNA-activated protein kinase, PKR	<i>Eif2ak2</i>	2.07E-02	1.39
Interferon-activable protein 205-B;Interferon-activable protein 205-A	<i>Ifi205b;Mnda;Ifi205a</i>	7.25E-03	1.35
E3 ubiquitin/ISG15 ligase TRIM25	<i>Trim25</i>	1.10E-02	1.35
Lymphocyte-specific protein 1	<i>Lsp1</i>	1.63E-02	1.34
Interferon regulatory factor 2-binding protein 2	<i>Irf2bp2</i>	6.92E-03	1.34
Interleukin-6 receptor subunit beta	<i>Il6st;il6st</i>	1.07E-02	1.25
Signal transducer and activator of transcription;Signal transducer and activator of transcription 3	<i>Stat3</i>	2.59E-02	1.17
Tripartite motif-containing protein 44	<i>Trim44</i>	2.02E-03	-10.82
CD97 antigen	<i>Adgre5;Cd97</i>	2.20E-03	-1.43
CD44 antigen	<i>Cd44</i>	1.20E-02	-1.43
CD302 antigen	<i>Cd302</i>	4.13E-02	-1.32
CD109 antigen	<i>Cd109</i>	1.22E-03	-1.31
Poliovirus Receptor	<i>Pvr</i>	1.23E-02	-1.26
Interferon regulatory factor 2-binding protein-like	<i>Irf2bpl</i>	1.56E-02	-1.21

Table 3: List of dysregulated factors in the innate immune system, ordered by direction of change (red for upregulations, dark green for downregulations) and by fold-changes. Among the many existing receptors for damage-associated-patterns, components of the pathways for detection of toxic DNA (highlighted by orange color) and double-stranded RNA (yellow) with their downstream nuclear transcription factors in the Stat-family (sky blue) were prominent among the upregulations. Plasma membrane epitopes (light green color) within the cluster of differentiation CD* superfamily stood out among the downregulations.

2.4 The strongest upregulations in *LonP1*^{+/−} MEFs can be seen in the lysosomal pathway

In the STRING analysis of all enrichments, “lysosome” was prominent among KEGG pathways (FDR = 1.19e-18), also among UNIPROT keywords (FDR = 1.18e-09) and among GO terms Molecular Function (FDR = 5.27e-09). Almost all dysregulations consisted in increased abundance of lysosomal factors, suggesting elevated degradation activity. This overactivity seemed directed towards specific targets, given that the strongest upregulations concerned the lysosomal cathepsin *Ctsc* as activator of many serine proteases in the immune system, and lysosomal cathepsin *Ctsz* also as a component of innate immune responses. Conversely, the strongest downregulation concerned the lysosomal cathepsin *Ctsh*, which is responsible for the overall degradation of proteins in lysosomes. While there was a strong increase for *Tmem59*, which directs endosomal LC3 labelling and lysosomal targeting, there was a reciprocal decrease for *Sqstm1* / p62, which directs protein aggregates to autophago-lysosomal degradation. It is also noteworthy that a dysregulation of the proteasomal pathways was not significant in STRING enrichment analysis. These findings could be interpreted as activated selective capacity for the vesicle-mediated elimination of mitochondrial fragments and other immune-response triggering bacteria by lysosomes. Indeed, among the GO terms Biological Process, there was a significant enrichment for “phagocytosis” (FDR = 0.0047), with upregulation of *Mesdc2*, *Colec12*, *Lrp1*, *Rab22a*, *B2m*, *Itgb3*, *Cdc42ep2* versus downregulation of *Mfge8*, *Axl*, *Thbs1*, *Rab31*, *Tgm2*, *Kif5b*, *Flnb*, *Anxa1*, *Anxa3*, *Myo1c*, *Cd302*, *Myh9*, *Gsn*, and *Vim*. As expected during innate immune responses, these changes were accompanied by massive changes in the REACTOME pathway “extracellular matrix organization” (FDR = 3.27e-15), in the KEGG pathway “focal adhesion” (9.94e-12) and in the INTERPRO protein domains “growth factor receptor cysteine-rich domain superfamily” (1.54e-05).

Protein names	Gene names	p-value	fold change
Dipeptidyl peptidase 1;Dipeptidyl peptidase 1 exclusion domain chain;Dipeptidyl peptidase 1 heavy chain;Dipeptidyl peptidase 1 light chain	<i>Ctsc</i>	5.62E-04	2.15
Transmembrane protein 59	<i>Tmem59</i>	1.62E-02	1.78
Cathepsin Z	<i>Ctsz</i>	1.46E-02	1.55
Alpha-mannosidase;Lysosomal alpha-mannosidase	<i>Man2b1</i>	9.63E-03	1.53
Beta-hexosaminidase;Beta-hexosaminidase subunit alpha	<i>Hexa</i>	3.15E-03	1.53
Sulfatase-modifying factor 1	<i>Sumf1</i>	3.30E-02	1.51
Alpha-galactosidase A	<i>Gla</i>	1.22E-02	1.48
Beta-glucuronidase	<i>Gusb</i>	3.24E-03	1.47
Type 1 phosphatidylinositol 4,5-bisphosphate 4-phosphatase	<i>Tmem55b</i>	5.30E-03	1.43
Cathepsin D	<i>Ctsd</i>	3.58E-04	1.41
Prosaposin	<i>Psap</i>	2.13E-02	1.41
Lysosomal thioesterase PPT2	<i>Ppt2</i>	4.56E-02	1.40
Putative phospholipase B-like 2;Putative phospholipase B-like 2 28 kDa form;Putative phospholipase B-like 2 40 kDa form;Putative phospholipase B-like 2 15 kDa form	<i>Plbd2</i>	4.65E-02	1.40
Carboxypeptidase;Lysosomal protective protein;Lysosomal protective protein 32 kDa chain;Lysosomal protective protein 20 kDa chain	<i>Ctsa</i>	4.80E-02	1.39
Granulins;Acrogranin;Granulin-1;Granulin-2;Granulin-3;Granulin-4;Granulin-5;Granulin-6;Granulin-7	<i>Grn</i>	1.66E-02	1.39
N-Acetyl-Alpha-Glucosaminidase	<i>Naglu</i>	6.52E-03	1.39
Lysosomal alpha-glucosidase	<i>Gaa</i>	7.20E-03	1.38
Arylsulfatase B	<i>Arsb</i>	2.36E-02	1.38
WD repeat-containing protein 59	<i>Wdr59</i>	1.10E-02	1.37
Beta-hexosaminidase;Beta-hexosaminidase subunit beta	<i>Hexb</i>	1.49E-02	1.37
Glucosylceramidase	<i>Gba</i>	5.95E-03	1.36
Gamma-glutamyl hydrolase	<i>Ggh</i>	1.12E-02	1.36
Beta-galactosidase	<i>Glb1</i>	4.01E-03	1.34
Cation-independent mannose-6-phosphate receptor	<i>Igf2r</i>	2.50E-03	1.33
Ganglioside GM2 activator	<i>Gm2a</i>	4.26E-04	1.32
Lysosomal Pro-X carboxypeptidase	<i>Prcp</i>	3.09E-02	1.25
Transmembrane protein 106B	<i>Tmem106b</i>	2.86E-02	1.25
Dipeptidyl peptidase 2	<i>Dpp7</i>	2.22E-02	1.24
Beta-mannosidase	<i>Manba</i>	2.15E-02	1.23
N(4)-(beta-N-acetylglucosaminy)-L-asparaginase;Glycosylasparaginase alpha chain;Glycosylasparaginase beta chain	<i>Aga</i>	1.23E-02	1.17
V-type proton ATPase subunit H	<i>Atp6v1h</i>	3.82E-02	1.17
Regulator complex protein LAMTOR1	<i>Lamtor1</i>	4.03E-02	1.14
AP-1 complex subunit beta-1;AP complex subunit beta	<i>Ap1b1</i>	1.84E-02	1.13
Pro-cathepsin H;Cathepsin H mini chain;Cathepsin H;Cathepsin H heavy chain;Cathepsin H light chain	<i>Ctsh</i>	8.68E-06	-1.73
Sequestosome-1	<i>Sqstm1</i>	9.12E-03	-1.23

Table 4: List of dysregulated factors in the lysosomal compartment, ordered by direction of change (red for upregulations, dark green for downregulations) and by fold-changes.

3. Discussion

This manuscript provides the first documentation of the global proteome of *LonP1*^{-/-} MEF. While a strong effect on oxidative processes in the mitochondria was expected and did not require validation, novel observations included the lack of mitoribosomal accumulations despite Eral1 accumulation. The *LonP1*^{-/-} proteome profile of all mitochondrially localized factors showed Eral1 as second highest upregulation. This was an unexpected finding, given that Eral1 was recently identified as a ClpXP degradation substrate [41]. Eral1 is a mitochondrial matrix chaperone, which associates with the small ribosomal subunit and contributes to mitoribosome assembly [68]. The complete unspecificity of Eral1 accumulation was confirmed in two meta-analyses of global proteome profiles, from *ClpP*^{-/-} heart and from ClpX overexpressing myoblasts. These meta-analyses indicate that mitoribosome accumulation occurs only upon CLPX mutations and correlates with ClpX levels.

In the bioinformatic analysis of the *LonP1*^{-/-} MEF global proteome, the previously published degradation substrates such as Aco2 and Tfam did not show changes in their protein abundances. Also, total mitochondrial biogenesis and mitophagy did not seem to be altered significantly. However, the lysosomal degradation of immunological targets was strongly upregulated together with phagocytosis and endosomal pathways, with the strongest upregulations concerning Ctsz and Ctsc which act in innate immune pathways [69, 70]. Furthermore, it seemed credible furthermore that *LonP1* deficiency affects the import of mitochondrial precursor proteins, since the mitochondrial import receptor Tomm70a, the import peptidase Pmpcb and the folding chaperone Hspd1 had significantly altered abundances. This is in good agreement with the previously established role of *LonP1* in the unfolded protein response [71, 72].

Several mitochondrial factors were significantly downregulated, which are involved in purine and pyrimidine synthesis, such as Mthfd1 and Dhodh, respectively [73, 74]. This contrasted with the strong upregulation of Abat, which is known for its role in the conversion of dNDPs to dNTPs. These findings again hint towards an altered RNA and DNA homeostasis in *LonP1*-deficient cells. In *ClpP*^{-/-} mice, we previously observed an accumulation of mtDNA [40], whereas mtDNA was lower upon knockdown of *LonP1* in B16F10 melanoma cells [30]. Both changes in content of mitochondrial DNA are accompanied by alterations of the innate immune system. In the *ClpP*^{-/-} mice, upregulations occur for several factors that are important in RIG-I signaling, which responds to viral RNA [40]. In *LonP1*-deficient cells, there were also upregulations of cytosolic factors responding to toxic RNA or DNA, such as Ifih1, Trim25, Mnda, Ifi204. Observations in both models, *ClpP* and *LonP1*, might reflect responses to the dysfunctional mitochondria and their altered state of nucleic acid content. It was recently shown that mitochondrial DNA or double-stranded RNA can escape to the cytosol and lead to cellular antiviral reactions [66, 67]. Since both systems that lack a mitochondrial matrix protease show features of changes of the innate immune system, this may be a general mechanism with mitochondrial dysfunction as an underlying cause. In contrast to *ClpP*^{-/-} mice, the *LonP1*^{-/-} MEF exhibited a significant downregulation of Trim44, which was shown to stabilize the mitochondrial antiviral signaling protein Mavs [75]. In regard to the lower amount of mtDNA upon *LonP1* deficiency, this downregulation could be a response towards the upregulation of other cytosolic nucleic acid sensors, as an effort of the cell to minimize the inflammatory state. This innate immune system activation was also documented in another model of mitochondrial dysfunction, where mice with deletion of the mitochondrial transcription factor Tfam display a massive induction of inflammatory signatures [67].

In the analysis of the global proteome of *LonP1*^{-/-} MEF beyond mitochondria, mostly upregulations were detected for pathways involved in oxidative stress and glutathione. The strongest upregulation was seen for Catalase, a factor known to play a major role in oxidative stress responses [76]. The second highest upregulation was seen for Sod3, which is also established as a marker for oxidative stress [77]. Other factors of the glutathione pathway, which is also involved in the neutralization of reactive oxidative species [78]. All these changes may reflect secondary cytoplasmic adaptations to altered oxidative processes in mitochondria.

Mitochondrial dysfunction is closely related to respiratory function. In chronically *ClpP*-deleted mice and cells there might be functional reductions in complex-I of the respiratory chain, but this

might be an indirect effect upon chronic tissue pathology [40, 41, 79]. In the acute knockdown of ClpP or ClpX, respiratory function of complex-II was selectively reduced [79, 80] and an accumulation of the subunits of complex-II was observed. In contrast, deficiency of LonP1 led to decreased activities of mitochondrial complex-I, III, and IV in heart tissue of LonP1 conditional knockout mice [81]. In LonP1^{+/-} mice heart complex-I levels and activities were decreased [82]. Mutations of LonP1 in humans lead to the rare multi-system developmental disorder - CODAS syndrome. Patients show swollen mitochondria with abnormal inner membrane morphology and reduced respiratory capacity [30]. Our results show that, in contrast to *ClpP*-deleted tissues, *LonP1*^{+/-} MEF exhibited upregulations for three proteins in the membrane arm of complex-I, namely Ndufa10, Ndubf7 and Ndubf4, whereas a slight downregulation was detected for one protein (Ndufa5) in the peripheral arm (Q-module) [83]. Given that LonP1 is localized in the matrix, the accumulation of the HP membrane arm may be due to an indirect effect, when a preassembled subcomplex consisting of the joint ND5, ND4 and ND2 module of the membrane arm cannot be docked onto an improperly folded Q module in the IP/FP matrix arm.

Lon protease function decreases with old age in mice. It was also seen that overexpression of the Lon protease orthologue in *P. anserina* resulted in a prolonged lifespan [84, 85]. This hints towards its role in the regulation of stress and survival [86]. Mitochondrial mutants and altered life expectancy are intimately related and have been most studied in *C. elegans* [87]. The homozygous deficiency of LonP1 shows one of the most drastic effects on lifespan, since mice die very early *in utero* and even the heterozygous depletion results in strong changes in various cellular processes. We could here show that there are similarities between the absence of ClpP and Lonp1, highlighting their crucial roles in protein homeostasis within mitochondria. But we also defined LonP1-deletion-specific consequences, so the relative targets of each protease may be inferred. Still, in order to understand all functions of ClpP and Lonp1, much future research will be needed.

4. Materials and Methods

Cell Culture:

The LonP1^{+/−} MEF have been generated and described before [6]. Cells were maintained in Dulbecco's minimal essential medium with 4.5 g/l glucose (Invitrogen) plus 15% fetal bovine growth serum (Gibco, One Shot), 1% Penicillin/Streptomycin (Gibco) and 1% Glutamine (Invitrogen) at 37 °C and 5% CO₂ in a humidified incubator, and were passaged every 3-4 days. All cell lines were regularly tested for Mycoplasma contamination.

Proteomics:

Protein abundance of cell pellets from LonP1^{+/−} MEF lines and their matching controls (n=3) were analyzed by label-free quantitative proteomics as recently described [88]. Mass spectrometry data were analysed by Max Quant [89] and extended statistics were done with Perseus [90]. Quantified proteins were quality filtered for at least 3 label free quantification values in one experimental group. Missing values were randomly replaced from normal distribution. Common contaminants and reverse identifications were excluded. For statistical comparison Student's t-tests were used.

Bioinformatic analyses:

For protein-protein-interaction (PPI) network analysis, the software tool STRING (Search tool for the retrieval of interacting genes) v.11.0 (<https://string-db.org/>) with standard settings was used to visualize networks among factors with >2-fold dysregulation in at least one of the three biological replicates [91]. Automated network statistics were performed; significant functional enrichments of GO (Gene Ontology terms regarding biological processes, molecular functions, cellular components), KEGG pathways, REACTOME pathways, PFAM protein domains, INTERPRO Protein Domains and Features, and SMART protein domains were exported into Excel files. Pathway findings were processed further into tables for dysregulated (p-values<0.05) mitochondrial factors, oxidative stress and glutathione factors, innate immunity factors as well as lysosomal factors.

Author Contributions: Conceptualization, G.A.; methodology, G.A., I.W., J.K., J.H. and A.K.; resources, C.L.-O. and C.B.; writing-original draft preparation, J.K., G.A., A.K. and I.W.; writing-review and editing, all authors.

Funding: This research was funded by the Deutsche Forschungsgemeinschaft (SFB815 Z1).

Acknowledgements: We thank Jana Meisterknecht for excellent technical assistance.

Conflicts of Interest: The authors declare no conflict of interest.

Abbreviations

AAA+	ATPases Associated with diverse cellular Activities
AFG3L2	AFG3-Like matrix AAA peptidase subunit 2
ATPase	Adenosine Tri-Phosphatase
CLPP	Caseinolytic Mitochondrial Matrix Peptidase Proteolytic Subunit
CLPX	Caseinolytic Mitochondrial Matrix Peptidase Chaperone Subunit
CO ₂	Carbon dioxide
CoA	Coenzyme-A
CODAS	Syndrome with cerebral, ocular, dental, auricular, and skeletal anomalies
DNA	Deoxyribonucleic acid
dNDPs	Deoxy-Nucleoside Di-Phosphate
dNTPs	Deoxy-Nucleoside Tri-Phosphate
dsRNA	Double-stranded RNA
FDR	False discovery rate
g	gram
GABA	Gamma-Amino Butyric Acid
GO	Gene Ontology

HP arm	Membrane hydrophobic part of respiratory complex I
INTERPRO	Database of protein families, domains and functional sites
IP/FP arm	Iron-sulfur-cluster containing part and FMN containing part of respiratory complex I
KEGG	Kyoto Encyclopedia of Genes and Genomes
KO	knockout
l	liter
LC3	Light Chain 3 protein, encoded by the <i>MAP1LC3A</i> gene
LIM-type	Zinc finger domain named after proteins LIN-11, Isl1 and MEC-3 where they were first found
LONP1	Mitochondrial ATP-Dependent Protease Lon, or PRSS15 for Serine Protease 15
MCU	Mitochondrial Calcium Uniporter
MEF	Murine embryonal fibroblasts
mAAA	Matrix AAA Peptidase
mtDNA	Mitochondrial DNA
NOD	Nucleotide-binding oligomerization domain-containing protein
PARK2	Autosomal recessively inherited Parkinson's disease type 2, caused by mutations in Parkin
PARK6	Autosomal recessively inherited Parkinson's disease type 6, caused by mutations in PINK1
PARK7	Autosomal recessively inherited Parkinson's disease type 7, caused by mutations in DJ-1
PARL	Presenilin-Associated Rhomboid-Like protein, mitochondrial protease
PFAM	Database of protein families including their annotations and multiple sequence alignments
PINK1	PTEN-induced Kinase 1, mitochondrial
PRLTS3	Perrault syndrome type 3 due to CLPP mutations
REACTOME	Database of reactions, pathways and biological processes
RIG-I	Retinoic Acid-Inducible Gene 1 Protein, encoded by the <i>Ddx58</i> gene
RNA	Ribonucleic acid
SCA28	Spinocerebellar Ataxia type 28, caused by mutations in
SMART	Simple Modular Architecture Research Tool
SMDT1	Single-pass Membrane protein with Aspartate-rich Tail 1, mitochondrial
STING	Stimulator of INterferon Genes protein, encoded by the <i>Tmem173</i> gene
STRING	Search tool for the retrieval of interacting genes
TCA cycle	Tricarboxylic acid cycle, Citric acid cycle, Krebs cycle
UPRmt	Mitochondrial Unfolded Protein Response
WT	wildtype

Appendix

Supplementary Table A1. *LonP1*^{+/−} mouse embryonal fibroblast global proteome profile via label-free mass spectrometry. Different data sheets show (i) contact information, (ii) sample information, (iii) methods employed, (iv) output data with a Volcano plot (where significant upregulations are shown in red color, significant downregulations in green, the mutant protein in blue, with significance scores on the Y-axis, fold-changes on the X-axis) and a list of detected peptides with relevant measures. Significance is scored as a nominal variant in column 9, significant upregulations are highlighted in column 10, significant downregulations in column 11, these proteins were analyzed further in STRING bioinformatics. Fold-changes are documented in column 8, p-values in column 6.

Supplementary Table A2. STRING analysis of enriched protein-protein interactions within the previously published global proteome profile of C2C12 myoblasts with ClpX overexpression [36]. Different datasheets present automated bioinformatics on defined (i) KEGG pathways, (ii) GO-terms Cellular Component, (iii) GO terms Biological Process, (iv) GO terms Molecular function, assigning statistical significance via false discovery rates (FDR values) in column D and identifying the dysregulated factors within each pathway in column F.

Supplementary Figure A1. Global proteome profile of *ClpX*-overexpressing myoblast cells. STRING diagram of interactions among proteins with >1.5-fold accumulation in myoblasts with ClpX

overexpression, as bioinformatics re-assessment of a dataset published previously [36]. Mitochondrial proteins are identified by bullets in red color. Prominent clusters reflect the accumulation of ClpX with mitochondrial Hspa9 (1.5-fold), Hspd1 (1.8-fold) and several extra-mitochondrial chaperones (highlighted by circle with pink background), as well as the accumulation of mitoribosomal proteins (between 2-fold and 1.1-fold, circle with green background), of proteins in the nucleolus as a pre-ribosome factory (circle with orange background), of proteins in the nuclear pore and in microtubule transport (circle with grey background) and of proteins within the mitochondrial import pore (clustered above and within the yellow circle).

References

1. Key, J. et al. (2019) Ubiquitylome profiling of Parkin-null brain reveals dysregulation of calcium homeostasis factors ATP1A2, Hippocalcin and GNA11, reflected by altered firing of noradrenergic neurons. *Neurobiol Dis* 127, 114-130.
2. Rugarli, E.I. and Langer, T. (2012) Mitochondrial quality control: a matter of life and death for neurons. *EMBO J* 31 (6), 1336-49.
3. Torres-Odio, S. et al. (2017) Progression of pathology in PINK1-deficient mouse brain from splicing via ubiquitination, ER stress, and mitophagy changes to neuroinflammation. *J Neuroinflammation* 14 (1), 154.
4. West, A.P. et al. (2011) Mitochondria in innate immune responses. *Nat Rev Immunol* 11 (6), 389-402.
5. Bulteau, A.L. and Bayot, A. (2011) Mitochondrial proteases and cancer. *Biochim Biophys Acta* 1807 (6), 595-601.
6. Quiros, P.M. et al. (2014) Lon protease: A key enzyme controlling mitochondrial bioenergetics in cancer. *Mol Cell Oncol* 1 (4), e968505.
7. Quiros, P.M. et al. (2015) New roles for mitochondrial proteases in health, ageing and disease. *Nat Rev Mol Cell Biol* 16 (6), 345-59.
8. Di Bella, D. et al. (2010) Mutations in the mitochondrial protease gene AFG3L2 cause dominant hereditary ataxia SCA28. *Nat Genet* 42 (4), 313-21.
9. Shendelman, S. et al. (2004) DJ-1 is a redox-dependent molecular chaperone that inhibits alpha-synuclein aggregate formation. *PLoS Biol* 2 (11), e362.
10. Torres-Odio, S. et al. (2017) Progression of pathology in PINK1-deficient mouse brain from splicing via ubiquitination, ER stress, and mitophagy changes to neuroinflammation. *Journal of neuroinflammation* 14 (1), 154.
11. Shi, G. and McQuibban, G.A. (2017) The Mitochondrial Rhomboid Protease PARL Is Regulated by PDK2 to Integrate Mitochondrial Quality Control and Metabolism. *Cell Rep* 18 (6), 1458-1472.
12. Valente, E.M. et al. (2004) Hereditary early-onset Parkinson's disease caused by mutations in PINK1. *Science* 304 (5674), 1158-60.
13. Exner, N. et al. (2007) Loss-of-function of human PINK1 results in mitochondrial pathology and can be rescued by parkin. *The Journal of neuroscience : the official journal of the Society for Neuroscience* 27 (45), 12413-8.
14. Gispert, S. et al. (2009) Parkinson phenotype in aged PINK1-deficient mice is accompanied by progressive mitochondrial dysfunction in absence of neurodegeneration. *PLoS One* 4 (6), e5777.
15. Gispert, S. et al. (2015) Potentiation of neurotoxicity in double-mutant mice with Pink1 ablation and A53T-SNCA overexpression. *Human molecular genetics* 24 (4), 1061-76.
16. Key, J. et al. (2019) Ubiquitylome profiling of Parkin-null brain reveals dysregulation of calcium homeostasis factors ATP1A2, Hippocalcin and GNA11, reflected by altered firing of noradrenergic neurons. *Neurobiology of disease* 127, 114-130.
17. Kitada, T. et al. (1998) Mutations in the parkin gene cause autosomal recessive juvenile parkinsonism. *Nature* 392 (6676), 605-8.
18. Wai, T. et al. (2016) The membrane scaffold SLP2 anchors a proteolytic hub in mitochondria containing PARL and the i-AAA protease YME1L. *EMBO reports* 17 (12), 1844-1856.
19. Sekine, S. et al. (2019) Reciprocal Roles of Tom7 and OMA1 during Mitochondrial Import and Activation of PINK1. *Molecular cell* 73 (5), 1028-1043 e5.
20. Hwang, A.B. et al. (2012) Mitochondria and organismal longevity. *Curr Genomics* 13 (7), 519-32.
21. Aerts, A.M. et al. (2009) Mitochondrial dysfunction leads to reduced chronological lifespan and increased apoptosis in yeast. *FEBS Lett* 583 (1), 113-7.

22. Fischer, F. et al. (2013) Human CLPP reverts the longevity phenotype of a fungal ClpP deletion strain. *Nat Commun* 4, 1397.
23. Bota, D.A. et al. (2002) Modulation of Lon protease activity and aconitase turnover during aging and oxidative stress. *FEBS Lett* 532 (1-2), 103-6.
24. Bota, D.A. and Davies, K.J. (2002) Lon protease preferentially degrades oxidized mitochondrial aconitase by an ATP-stimulated mechanism. *Nat Cell Biol* 4 (9), 674-80.
25. Fu, G.K. and Markovitz, D.M. (1998) The human LON protease binds to mitochondrial promoters in a single-stranded, site-specific, strand-specific manner. *Biochemistry* 37 (7), 1905-9.
26. Lu, B. et al. (2003) The ATP-dependent Lon protease of *Mus musculus* is a DNA-binding protein that is functionally conserved between yeast and mammals. *Gene* 306, 45-55.
27. Gur, E. and Sauer, R.T. (2008) Recognition of misfolded proteins by Lon, a AAA(+) protease. *Genes Dev* 22 (16), 2267-77.
28. Peter, B. et al. (2018) Defective mitochondrial protease LonP1 can cause classical mitochondrial disease. *Human molecular genetics* 27 (10), 1743-1753.
29. Dikoglu, E. et al. (2015) Mutations in LONP1, a mitochondrial matrix protease, cause CODAS syndrome. *American journal of medical genetics. Part A* 167 (7), 1501-9.
30. Strauss, K.A. et al. (2015) CODAS syndrome is associated with mutations of LONP1, encoding mitochondrial AAA+ Lon protease. *American journal of human genetics* 96 (1), 121-35.
31. Fukuda, R. et al. (2007) HIF-1 regulates cytochrome oxidase subunits to optimize efficiency of respiration in hypoxic cells. *Cell* 129 (1), 111-22.
32. Granot, Z. et al. (2007) Turnover of mitochondrial steroidogenic acute regulatory (StAR) protein by Lon protease: the unexpected effect of proteasome inhibitors. *Mol Endocrinol* 21 (9), 2164-77.
33. Tian, Q. et al. (2011) Lon peptidase 1 (LONP1)-dependent breakdown of mitochondrial 5-aminolevulinic acid synthase protein by heme in human liver cells. *J Biol Chem* 286 (30), 26424-30.
34. Lu, B. et al. (2013) Phosphorylation of human TFAM in mitochondria impairs DNA binding and promotes degradation by the AAA+ Lon protease. *Mol Cell* 49 (1), 121-32.
35. Baker, T.A. and Sauer, R.T. (2012) ClpXP, an ATP-powered unfolding and protein-degradation machine. *Biochim Biophys Acta* 1823 (1), 15-28.
36. Al-Furoukh, N. et al. (2015) ClpX stimulates the mitochondrial unfolded protein response (UPRmt) in mammalian cells. *Biochimica et biophysica acta* 1853 (10 Pt A), 2580-91.
37. Haynes, C.M. et al. (2007) ClpP mediates activation of a mitochondrial unfolded protein response in *C. elegans*. *Dev Cell* 13 (4), 467-80.
38. Andersson, F.I. et al. (2009) Structure and function of a novel type of ATP-dependent Clp protease. *J Biol Chem* 284 (20), 13519-32.
39. Jenkinson, E.M. et al. (2013) Perrault syndrome is caused by recessive mutations in CLPP, encoding a mitochondrial ATP-dependent chambered protease. *Am J Hum Genet* 92 (4), 605-13.
40. Gispert, S. et al. (2013) Loss of mitochondrial peptidase Clpp leads to infertility, hearing loss plus growth retardation via accumulation of CLPX, mtDNA and inflammatory factors. *Human molecular genetics* 22 (24), 4871-87.
41. Szczepanowska, K. et al. (2016) CLPP coordinates mitochondrial assembly through the regulation of ERAL1 levels. *The EMBO journal* 35 (23), 2566-2583.
42. Jin, S.M. and Youle, R.J. (2013) The accumulation of misfolded proteins in the mitochondrial matrix is sensed by PINK1 to induce PARK2/Parkin-mediated mitophagy of polarized mitochondria. *Autophagy* 9 (11), 1750-7.
43. Horner, S.M. et al. (2015) Proteomic analysis of mitochondrial-associated ER membranes (MAM) during RNA virus infection reveals dynamic changes in protein and organelle trafficking. *PLoS One* 10 (3), e0117963.
44. Zhang, W. et al. (2019) Lactate Is a Natural Suppressor of RLR Signaling by Targeting MAVS. *Cell*.
45. Key, J. et al. (in submission) Loss of mitochondrial peptidase ClpP triggers transcriptional induction of Rnf213, a susceptibility factor for Moyamoya disease.
46. Quiros, P.M. et al. (2014) Lon protease: A key enzyme controlling mitochondrial bioenergetics in cancer. *Molecular & cellular oncology* 1 (4), e968505.
47. Lu, B. et al. (2013) Phosphorylation of human TFAM in mitochondria impairs DNA binding and promotes degradation by the AAA+ Lon protease. *Molecular cell* 49 (1), 121-32.
48. Gibellini, L. et al. (2015) Inhibition of Lon protease by triterpenoids alters mitochondria and is associated to cell death in human cancer cells. *Oncotarget* 6 (28), 25466-83.
49. Li, P.A. et al. (2017) Mitochondrial biogenesis in neurodegeneration. *Journal of neuroscience research* 95 (10), 2025-2029.
50. Villa, E. et al. (2018) No Parkin Zone: Mitophagy without Parkin. *Trends in cell biology* 28 (11), 882-895.

51. Escobar-Henriques, M. and Joaquim, M. (2019) Mitofusins: Disease Gatekeepers and Hubs in Mitochondrial Quality Control by E3 Ligases. *Frontiers in physiology* 10, 517.
52. Sun, S. et al. (2019) Long Noncoding RNA LINC00265 Promotes Glycolysis and Lactate Production of Colorectal Cancer through Regulating of miR-216b-5p/TRIM44 Axis. *Digestion*, 1-10.
53. Yang, B. et al. (2013) Novel function of Trim44 promotes an antiviral response by stabilizing VISA. *Journal of immunology* 190 (7), 3613-9.
54. Hoshino, A. et al. (2014) Oxidative post-translational modifications develop LONP1 dysfunction in pressure overload heart failure. *Circulation. Heart failure* 7 (3), 500-9.
55. Leiser, S.F. et al. (2015) Cell nonautonomous activation of flavin-containing monooxygenase promotes longevity and health span. *Science* 350 (6266), 1375-1378.
56. Wirth, C. et al. (2016) Structure and function of mitochondrial complex I. *Biochimica et biophysica acta* 1857 (7), 902-14.
57. Bross, P. and Fernandez-Guerra, P. (2016) Disease-Associated Mutations in the HSPD1 Gene Encoding the Large Subunit of the Mitochondrial HSP60/HSP10 Chaperonin Complex. *Frontiers in molecular biosciences* 3, 49.
58. Greene, A.W. et al. (2012) Mitochondrial processing peptidase regulates PINK1 processing, import and Parkin recruitment. *EMBO reports* 13 (4), 378-85.
59. Vogtle, F.N. et al. (2018) Mutations in PMPCB Encoding the Catalytic Subunit of the Mitochondrial Presequence Protease Cause Neurodegeneration in Early Childhood. *American journal of human genetics* 102 (4), 557-573.
60. Besse, A. et al. (2015) The GABA transaminase, ABAT, is essential for mitochondrial nucleoside metabolism. *Cell metabolism* 21 (3), 417-27.
61. Richard, H.T. and Foster, J.W. (2003) Acid resistance in *Escherichia coli*. *Advances in applied microbiology* 52, 167-86.
62. Nilsson, G.E. and Lutz, P.L. (2004) Anoxia tolerant brains. *Journal of cerebral blood flow and metabolism : official journal of the International Society of Cerebral Blood Flow and Metabolism* 24 (5), 475-86.
63. Wagener, N. and Neupert, W. (2012) Bcs1, a AAA protein of the mitochondria with a role in the biogenesis of the respiratory chain. *Journal of structural biology* 179 (2), 121-5.
64. Hornig-Do, H.T. et al. (2012) Nonsense mutations in the COX1 subunit impair the stability of respiratory chain complexes rather than their assembly. *The EMBO journal* 31 (5), 1293-307.
65. Konig, T. et al. (2016) The m-AAA Protease Associated with Neurodegeneration Limits MCU Activity in Mitochondria. *Molecular cell* 64 (1), 148-162.
66. Dhir, A. et al. (2018) Mitochondrial double-stranded RNA triggers antiviral signalling in humans. *Nature* 560 (7717), 238-242.
67. West, A.P. et al. (2015) Mitochondrial DNA stress primes the antiviral innate immune response. *Nature* 520 (7548), 553-7.
68. Uchiumi, T. et al. (2010) ERAL1 is associated with mitochondrial ribosome and elimination of ERAL1 leads to mitochondrial dysfunction and growth retardation. *Nucleic Acids Res* 38 (16), 5554-68.
69. Herias, V. et al. (2015) Leukocyte cathepsin C deficiency attenuates atherosclerotic lesion progression by selective tuning of innate and adaptive immune responses. *Arterioscler Thromb Vasc Biol* 35 (1), 79-86.
70. Campden, R.I. and Zhang, Y. (2019) The role of lysosomal cysteine cathepsins in NLRP3 inflammasome activation. *Arch Biochem Biophys*.
71. Pareek, G. and Pallanck, L.J. (2018) Inactivation of Lon protease reveals a link between mitochondrial unfolded protein stress and mitochondrial translation inhibition. *Cell Death Dis* 9 (12), 1168.
72. Bezawork-Geleta, A. et al. (2015) LON is the master protease that protects against protein aggregation in human mitochondria through direct degradation of misfolded proteins. *Sci Rep* 5, 17397.
73. Hum, D.W. et al. (1988) Primary structure of a human trifunctional enzyme. Isolation of a cDNA encoding methylenetetrahydrofolate dehydrogenase-methenyltetrahydrofolate cyclohydrolase-formyltetrahydrofolate synthetase. *J Biol Chem* 263 (31), 15946-50.
74. Löffler, M. et al. (1997) Dihydroorotat-ubiquinone oxidoreductase links mitochondria in the biosynthesis of pyrimidine nucleotides. *Mol Cell Biochem* 174 (1-2), 125-9.
75. Yang, B. et al. (2013) Novel function of Trim44 promotes an antiviral response by stabilizing VISA. *J Immunol* 190 (7), 3613-9.
76. Rohrdanz, E. et al. (2001) The influence of oxidative stress on catalase and MnSOD gene transcription in astrocytes. *Brain Res* 900 (1), 128-36.
77. Wang, Y. et al. (2018) Superoxide dismutases: Dual roles in controlling ROS damage and regulating ROS signaling. *J Cell Biol* 217 (6), 1915-1928.
78. Sies, H. (1999) Glutathione and its role in cellular functions. *Free Radic Biol Med* 27 (9-10), 916-21.

79. Cole, A. et al. (2015) Inhibition of the Mitochondrial Protease ClpP as a Therapeutic Strategy for Human Acute Myeloid Leukemia. *Cancer Cell* 27 (6), 864-76.
80. Seo, J.H. et al. (2016) The Mitochondrial Unfoldase-Peptidase Complex ClpXP Controls Bioenergetics Stress and Metastasis. *PLoS Biol* 14 (7), e1002507.
81. Lu, B. et al. LonP1 Orchestrates UPRmt and UPRER and Mitochondrial Dynamics to Regulate Heart Function. *BioRxiv*, The preprint server for biology.
82. Venkatesh, S. et al. (2019) Mitochondrial LonP1 protects cardiomyocytes from ischemia/reperfusion injury in vivo. *J Mol Cell Cardiol* 128, 38-50.
83. Stroud, D.A. et al. (2016) Accessory subunits are integral for assembly and function of human mitochondrial complex I. *Nature* 538 (7623), 123-126.
84. Bota, D.A. et al. (2005) Downregulation of the human Lon protease impairs mitochondrial structure and function and causes cell death. *Free Radic Biol Med* 38 (5), 665-77.
85. Luce, K. and Osiewacz, H.D. (2009) Increasing organismal healthspan by enhancing mitochondrial protein quality control. *Nat Cell Biol* 11 (7), 852-8.
86. Ngo, J.K. and Davies, K.J. (2007) Importance of the lon protease in mitochondrial maintenance and the significance of declining lon in aging. *Ann N Y Acad Sci* 1119, 78-87.
87. Yang, W. and Hekimi, S. (2010) Two modes of mitochondrial dysfunction lead independently to lifespan extension in *Caenorhabditis elegans*. *Aging Cell* 9 (3), 433-47.
88. Altmann, C. et al. (2016) Progranulin overexpression in sensory neurons attenuates neuropathic pain in mice: Role of autophagy. *Neurobiology of disease* 96, 294-311.
89. Cox, J. and Mann, M. (2008) MaxQuant enables high peptide identification rates, individualized p.p.b.-range mass accuracies and proteome-wide protein quantification. *Nature biotechnology* 26 (12), 1367-72.
90. Tyanova, S. et al. (2016) The Perseus computational platform for comprehensive analysis of (prote)omics data. *Nature methods* 13 (9), 731-40.
91. Franceschini, A. et al. (2013) STRING v9.1: protein-protein interaction networks, with increased coverage and integration. *Nucleic acids research* 41 (Database issue), D808-15.